

The Effects of a Synbiotic Diet on Humerus Bone Mineralization and Mechanical Strength in Aging Male Mice

Chandler Allen Sparks, Zachary T Giltner, Cynthia A Blanton, and Annette M Gabaldón

ABSTRACT

Previous studies suggest that probiotic-enhanced diets improve mineral absorption in the large intestine and are thus protective against bone mineral loss. A synbiotic diet, composed of both probiotics and prebiotics, may be even more effective because the bacteria can readily metabolize the fibers of the prebiotics to promote the growth and synthesis of secondary metabolites. We sought to investigate the long-term effects of a synbiotic diet on adult male retired breeder mice. We found that a synbiotic diet does not influence the bone mineralization of the humerus bone. Furthermore, we found that the synbiotic diet does not influence the mechanical strength properties (extrinsic stiffness, ultimate force, fracture force, energy to fracture) of the humerus bone. This study was a subproject of a larger investigation that assessed the influence of the synbiotic diet on femur and tibia bones of the same mice, which revealed similar findings.

El Rio: A Student Research Journal. Vol. 4, No. 1 (2021), pp. 3-10.

CC-BY Chandler Allen Sparks, et al. Colorado State University Library, Pueblo, CO, 81001.

Introduction

A synbiotic diet is composed of both prebiotics and probiotics. Probiotics are live microorganisms that are proposed to confer benefits to the host when consumed, such as the bacterial strains *Lactobacillus acidophilus* and *Lactococcus lactis lactis*. Prebiotics are non-digestible food components that support the growth and activity of bacteria in the gastrointestinal tract. Fructooligosaccharides meet the criteria to be classified as prebiotics. The addition of prebiotics to probiotics, i.e., a synbiotic diet, has been shown to increase the activity of the selected probiotic strains (Schrezenmeir and de Vrese 2001). This increase in activity leads to an increase in the production of short chain fatty acids by the probiotic strains (Scholz-Ahrens & Schrezenmeir 2002). The short chain fatty acids lower the intestinal pH, making minerals more soluble and therefore, more readily absorbed (Scholz-Ahrens & Schrezenmeir 2002). This increased activity of the probiotic strains also leads to an increase in the production of vitamins by the microbes that can be used to maintain bone health (Gibson et al. 1995). Additionally, a synbiotic diet has been shown to promote enterocyte growth, leading to an increased intestinal lining surface area for nutrients, including minerals, to be absorbed; this has been shown in both chickens (Sobolewska et al. 2017) and rats (Campbell et al. 1997).

Previous studies have investigated the effects of a synbiotic diet on bone health using various animal models to determine if mineralization and mechanical strength are enhanced. Scholz-Ahrens et al. 2002 reported that a diet supplemented with prebiotics (oligofructose) prevented the loss of bone mineral content in the femur bones of an ovariectomized female rat model. The effects of probiotic and prebiotic diets in human studies have mixed results, with some indicating no effect on mineral absorption (Ellegård et al. 1997; López-Huertas et al. 2006; Tahiri et al. 2003) and others indicating a positive influence on mineral absorption (Coudray et al. 1997; Van den Heuvel et al. 1999; Van den Heuvel et al. 2000).

Mice are commonly used for bone research because they share basic bone characteristics with humans, have a short gestation period, have high reproductive capabilities, and can be genetically altered (Jilka 2013). For example, age-related BMD loss, as experienced by some older human adults, also occurs in mice (Piemontese et al. 2017). In humans, age-related bone fragility has been associated with alterations in collagen composition (Wang et al. 2002) as well as the size of hydroxyapatite crystals (Cowin 2001). Abnormally thin collagen fibers (Bullough 1981), minerals outside of collagen fibrils (Vetter et al. 1991), altered organization of collagen fibers (Silva et al. 2005), and larger hydroxyapatite crystal size (Cowin 2001) have all been associated with bone fragility. Similar changes in collagen composition (Silva et al. 2005) and hydroxyapatite crystals (Freeman et al. 2001) have been observed in mice, also leading to bone fragility.

Here, we investigated the effects of a long-term synbiotic diet on bone mineralization and strength in adult male retired breeder mice. We previously investigated the influence of a synbiotic diet on two hindlimb bones (femur and tibia), which were collected from the same mice used in the present study, and those results were reported in a thesis project by Choman, 2015. Choman performed three-point bending tests to evaluate bone shaft mechanical strength and used micro-computed tomography to investigate microanatomical properties. Choman's major results showed that the adult male retired breeder mice fed the long-term synbiotic diet for four months did not demonstrate enhanced bone mineralization or mechanical strength. We sought to determine if the major findings from Choman's study, i.e., the absence of a synbiotic diet-induced bone enhancement, could be repeated using a different bone - the humerus bone from the forelimb. Thus, this subproject sought to confirm the findings of Choman, demonstrate that the three-point bending machine was suitable for testing small forelimb bones from mice, and taught undergraduate researchers in the CBASE program at Colorado State University Pueblo research techniques using the DEXA scanner as well as the three-point bending machine.

Methods

Animal Experimental Groups

Thirty 10-month-old male retired breeder mice (HSD: ICR (CD-1), Harlan Laboratories), were randomly divided into three groups (n=10 each): baseline (BSL), control (CON), and synbiotic (SYN). The mice were housed at Idaho State University (ISU) and the experimental protocol was approved by IACUC at Idaho State University, Pocatello. The animals were inspected for health on a daily basis and the study was conducted under veterinary supervision. No health problems developed in response to the diets and all animals completed the study. All mice were fed a standard mouse pelleted diet provided by the vendor. Upon receipt, they

were started on the control diet described in Table 1. The BSL group was kept on the control diet for two weeks before sacrifice. The CON group was fed the control diet for four months and sacrificed at age 14 months. The SYN group fed the control diet enhanced with synbioics for four months and sacrificed also at age 14 months. The BSL group served as a control to identify age-related changes of the bone, as it was sacrificed 3.5 months before the other groups. The CON group served as a control to identify synbiotic diet-induced changes in the bone.

Animal Diets

The control and synbiotic diet compositions are described in Table 1. All mice were fed an isocaloric diet with an energy density of 3800 kilocalories/kg diet. Mice in the BSL and CON group were fed a powdered form of the American Institute of Nutrition (AIN)-93M purified laboratory diet (*Dyets, Inc.*, Bethlehem, PA). Mice in the SYN group received the same diet but enhanced with synbiotics. All diets were prepared in by *Dyets Inc.*, Bethlehem, PA. The diets were in powder form so that food intake could be monitored, so mice were provided with Nalgene chew sticks to maintain dental health. The probiotic strains *Lactobacillus acidophilus* and *Lactococcus lactis lactis* (Nutraceutix, Redmond, Washington) comprised a total of 1% of the synbiotic diet's weight while the prebiotic fructooligosaccharide comprised 3% of the synbiotic diet's weight.

Table 1. Composition of control and synbiotic diets fed to mice.

Ingredient	Control (g / kg)	Synbiotic (g / kg)
Casein	140	140
Cellulose	50	24.5
Choline Bitartrate	2.5	2.5
Cornstarch	720.692	704.692
Fructooligosaccharide (prebiotic)	0	31.5
L-Cystine	1.8	1.8
Probiotic*	0	10
Salt Mix #210050	35	35
Soybean Oil	40	40
t-Butylhydroquinone	0.008	0.008
Vitamin Mix #210025	10	10

* Probiotic strains *Lactobacillus acidophilus* and *Lactococcus lactis lactis*

Bone Dissection

BSL group mice were euthanized at 10 months of age. The right forelimb was carefully removed from the glenoid fossa of the scapula, fixed in formalin, then stored in 70% ethanol and transported to Colorado State University Pueblo. Unintentionally, one left forelimb (rather than right) was removed from one BSL animal (BSL-3) but was kept for analysis. SYN and CON mice were euthanized at 14 months of age and the right forelimb was removed then stored as described for the BSL group. Incidentally, four humerus bones were found to be broken from the dissection (BSL-5, BSL-9, SYN-2, and SYN-3). These bones were used for DEXA scanning but could not be used in the three-point bending tests. The animal group size of $n = 10$ mice per group allows for these incidents in animal studies, as a group size of $n = 7-8$ is appropriate for statistical analysis. Prior to experimentation with the bones, all adhering soft tissue was removed, the humerus was separated from the radius and ulna, and the bones were hydrated in 0.9% saline solution for 24 hours.

Humerus Bone Mineral Density Measurements

Dual energy X-ray absorptiometry (DEXA) scanning is the most commonly used method for measuring the BMD of small animals used in studies of metabolic bone disease (Shi et al. 2016). The method is fast, low-radiation, and relatively inexpensive, making it the method of choice for researchers. DEXA scanners work by sending low-dose X-rays through a sample. The X-rays are absorbed differently by bones and soft tissues. Bone mineral content (BMC) and area of bone are determined by the amount of X-ray energy that is absorbed by the bone (Berger 2002). The denser the bone is, the less X-ray energy will pass through the bone and reach the detector. The values of BMC and area can then be used to determine BMD. The Lunar Piximus II DEXA scanner (Figure 1A) was developed specifically for measuring BMD in small animals and was used in the present study on dissected humeri bones.

All of the bones from each group, with a cotton thread and numbered label tied around each bone for identification, were placed on an artificial tissue block and scanned using the Lunar Piximus II DEXA scanner (Figure 1B). Following scanning, BMC (g), area (cm²), and BMD (g/cm²) values were obtained for individual bones by adjusting the region of interest (ROI) to capture a single bone (Figure 1C-D). The bones were analyzed in duplicate and the values from each measurement were averaged. Quality control testing, as described in the Lunar Piximus II DEXA scanner manual, was performed prior to use of the DEXA scanner to ensure accuracy of the measurements.

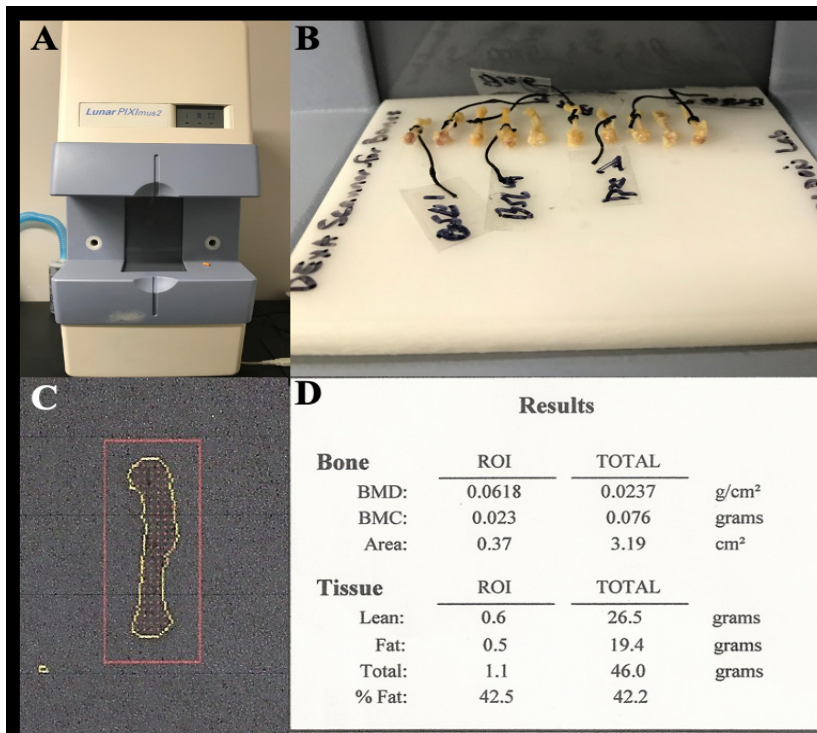


Figure 1. An example of a DEXA scan experiment. (A) The Lunar Piximus II DEXA scanner that was used in the present study. (B) Humeri bones from the BSL group placed on the artificial tissue block with a cotton thread and numbered label tied around them. (C) A single mouse humerus bone captured by the Lunar Piximus II DEXA scanner and enclosed in a ROI (red) for analysis. (D) A data report for the humerus bone shown in panel C.

Humerus Bone Mechanical Strength Testing

Three-point bending is a common method used to determine the mechanical properties of materials, including skeletal long bones, and was the method used here to determine strength properties of mouse humeri bones. Three-point bending is a beam loading method with two fixed supports and a point force in the middle. A three-point bending machine constructed by the Colorado State University Pueblo Department of Engineering and modified for mouse bones was used for mechanical strength testing (Figure 2A). The machine was equipped with a calibrated iLoad Mini force sensor, model MFM-010-050-S (LoadStar Sensors, Fremont, California) with 10 lb capacity and 1.0% accuracy, and a Mitutoyo displacement sensor, model ID-S112EX (Mitutoyo, Aurora, Illinois) with 0.001 mm resolution and 0.00012 inch accuracy. The sensors were connected to the same computer through a 24-bit load cell interface, model DQ-1000 (LoadStar Sensors, Fremont, California). Also, an Exttech Instruments external power source, model 382213 (Exttech Instruments, Nashua, New Hampshire) was connected to the machine to supply power.

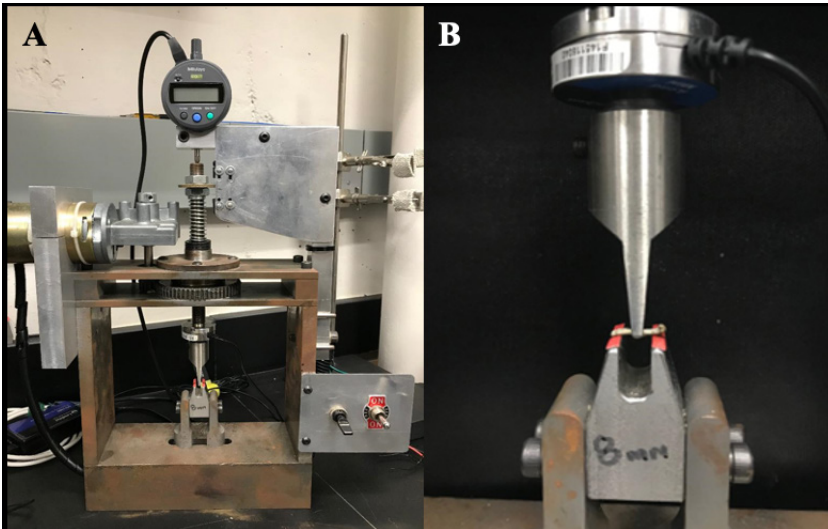


Figure 2. The three-point bending machine utilized in the present study. (A) The three-point bending machine imaged with deflection meter and force sensor. (B) A humerus bone on a two-beam support with crosshead beam at the midshaft.

All humerus bones were placed on a two-beam support with an 8.0 mm width from beam center-to-center (Figure 2B). The posterior surface of the bone was positioned upward, facing the crosshead beam. The top surfaces of the support beams were covered with 80-grit sandpaper to ensure that the bones did not shift during the mechanical strength testing. The crossbeam lowering speed was ensured to be at 1 ± 0.05 mm per minute prior to each day of testing. A preload force of 0.5 – 1.0 N was applied to each bone at the start of each test to help stabilize the bone and ensure a common starting point between different tests. Baseline data, with a preload applied, was collected for 5 seconds prior to further lowering the crosshead beam onto the bone and for 5 seconds following complete fracture of the bone. Data were logged from SensorVue software to Excel in real time and later transferred to Igor Pro 6.36 for analysis of the force-displacement curves. A representative curve analysis procedure is shown in Figure 3. The cursor placements correspond to regions of interest for the various mechanical properties of interest (extrinsic stiffness, ultimate force, fracture force, and energy to fracture). For example, the area under the curve for cursor pair A-B is fracture energy absorbed (N*mm). The slope of the curve between cursor pair C-D is the extrinsic stiffness. These and other relationships are summarized in Table 2. Each force-displacement curve generated by a single humerus bone was analyzed in duplicate and the values from each analysis were averaged.

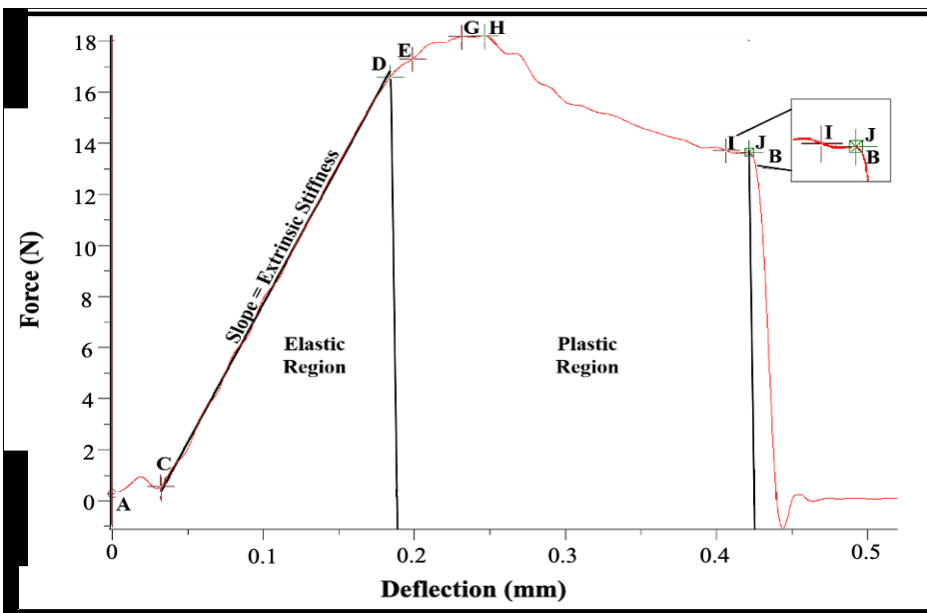


Figure 3. A representative force-deflection curve for a 3-point bending test on a mouse humerus bone. The curves were generated and analyzed using waveform analysis tools in Igor Pro 6.36. Cursors were placed on the force-displacement curve to mark regions of interest. The entire curve is bound by cursors A and B. Cursors C and D identify the linear elastic region, the portion of the curve where the bone will return to its original shape if the force is removed. Cursor E marks the yield point, the point beyond which the bone becomes plastic, where it will not return to its original shape if the force is removed. Cursors G and H bracket the ultimate force. Cursors I and J bracket the fracture force region.

Table 2. Regions defined by cursors and corresponding mechanical properties for force-deflection

Mechanical Property	Cursors	Measurement
Extrinsic stiffness (N/mm)	C-D	Slope
Ultimate force (N)	G-H	Average of points
Fracture force (N)	I-J	Average of points
Fracture energy absorbed (N*mm)	A-B	Area underneath curve

Statistical analyses

Within the general linear, least squares fit model, One-way analysis of variance (ANOVA) was used to analyze main effects of group on DEXA (BMC, bone area, and BMD) and mechanical strength (extrinsic stiffness, ultimate force, fracture force, and energy to fracture) variables. Whenever a significant main effect was found, post-hoc multiple comparisons were performed using Tukey's HSD and Student's t test. Results are reported as means \pm standard error of the mean (SEM) and differences were considered significant at $p < 0.05$. Statistical analyses were performed using JMP Pro®, Version 15.20, SAS Institute Inc., Cary, NC.

Results

Humerus bone mineralization

BMD, BMC, and area for BSL (n=10), CON (n=10), and SYN (n=10) mice were successfully obtained using the DEXA scanner and mean \pm SEM values are shown in Table 3. One-way ANOVA revealed a significant main effect of group on BMC ($p = 0.0075$) and area ($p < 0.0001$). Post-hoc analysis using a student's t-test revealed significant differences in BMC for SYN vs. BSL (10% lower in SYN, $p = 0.0245$) and SYN vs. CON (13% lower in SYN, $p = 0.0025$), but no difference for BSL vs. CON ($p = 0.3492$). Post-hoc analysis using a more rigorous Tukey's test also revealed a significant difference in BMC for SYN vs. CON ($p = 0.0068$) and near significance for SYN vs. BSL ($p = 0.0615$). Similar results were observed for post-hoc comparisons of bone area values which were significantly lower in SYN vs. BSL and CON groups. Specifically, bone area was 10.5% less in SYN vs. BSL (Student's t test, $p < 0.0001$; Tukey's, $p < 0.0001$) and 12% less in SYN vs. CON (Student's t test, $p < 0.0001$; Tukey's, $p < 0.0001$). One-way ANOVA did not reveal a main effect on BMD ($p = 0.7467$), thus all groups had values that were not significantly different.

Table 3. Mouse humerus bone DEXA scanning measurements of BMD, BMC, and bone area.

Group	BMD (g/cm ²)	BMC (g)	Area (cm ²)
BSL, 10 mo	0.05533 \pm 0.00098 A	0.0202 \pm 0.0006A	0.370 \pm 0.00424 A
CON, 14 mo	0.05632 \pm 0.00095 A	0.0210 \pm 0.00062A	0.376 \pm 0.00587 A
SYN, 14 mo	0.05517 \pm 0.00409 A	0.0182 \pm 0.00046B	0.331 \pm 0.00837 B
Main Effect Group, p-Value			
(One-Way ANOVA)	$p = 0.7467$	$p = 0.0075^*$	$p < 0.0001^*$

Values are means \pm SEM. *One-way ANOVAs with post-hoc multiple comparisons shown for Student's t-test. Within a column, values not sharing a letter superscript are significantly different ($p < 0.05$).

Humerus bone mechanical strength properties

From the force-displacement curves generated using three-point bending, intrinsic stiffness, ultimate force, fracture force, and energy to fracture were obtained for BSL (n=8), CON (n=10), and SYN (n=8) mice. The results are summarized in Table 4. One-way ANOVA showed no main effect of group on extrinsic stiffness ($p = 0.2392$), ultimate force ($p = 0.2160$), fracture force ($p = 0.3877$), or energy to fracture ($p = 0.5122$), thus all groups had values that were not significantly different.

Table 4. Average intrinsic stiffness, ultimate force, fracture force, and energy to fracture of mouse humerus bones obtained from three-point bending.

Group	Extrinsic Stiffness (N/mm)	Ultimate Force (N)	Fracture Force (N)	Energy to Fracture (N*mm)
BSL, 10 mo	127.90±33.50	16.28±0.51	16.29±0.55	2.56±0.39
CON, 14 mo	106.53±4.78	18.05±0.80	17.71±0.97	2.53±0.19
SYN, 14 mo	139.99±30.68	17.83±0.69	17.83±0.69	2.75±0.29
Main Effect Group, p-Value				
(One-Way ANOVA)	p = 0.2392	p = 0.2160	p = 0.3877	p = 0.5122

Values are means ± SEM. *One-way ANOVAs showed no main effects of group for any variable.

Discussion

The goal of this study was to determine the effects of a long-term synbiotic diet on skeletal bone mineral density and mechanical strength in adult male retired breeder mice fed the diet from ages 10 to 14 months. We found that the synbiotic diet did not have a significant effect on BMD, which indicates that the diet likely did not influence mineralization in the mice. Mice in the synbiotic diet group did, however, have significantly lower BMC (10-13% less) and bone area (10.5-12% less) compared to mice in the other groups, which suggests that they have moderately smaller humerus bones. Possibly, the synbiotic diet induced microanatomical changes in the bone cortical surface area. This possibility could be determined in future studies using high resolution imaging such as micro-computed tomography. Of the three-point bending test parameters analyzed, ultimate force and fracture force are measures of strength. The finding that the synbiotic diet did not influence either of these two variables thus indicates that it does not influence strength. Furthermore, the synbiotic diet did not influence the humerus bone's extrinsic stiffness or energy to fracture.

The findings of this study are consistent with those of Choman (2015), who analyzed the femur bones from the same mice used in the present study. Choman showed that a synbiotic diet did not provide mechanical strength benefits and was associated with slightly decreased BMD. Choman showed this using a three-point bending machine and micro-computed tomography. It should be noted, however, that there were changes in the geometry of the femur bones in mice fed the synbiotic diet, as analyzed by micro-computed tomography scanning (Choman, 2015). The findings of this study, however, do differ from those of similar studies with different animals. As noted, Scholz-Ahrens et al. have shown positive results of the diet on bone health in rats (Scholz-Ahrens et al. 2002). Some human studies show positive effects of the diet (Coudray et al. 1997; Van den Heuvel et al. 1999; Van den Heuvel et al. 2000) with others showing no effect ((Ellegård et al. 1997; López-Huertas et al. 2006; Tahiri et al. 2003). The mixed results of studies regarding probiotics, prebiotics, and a synbiotic diet in rats, mice, and humans may indicate that the diet has different influences on different species. Future works regarding the variation of bone response to a synbiotic diet between species and individuals will need to be conducted to address this.

The mice used in this study were male albino breeder mice that were purchased at 10 months of age (BSL) and fed the synbiotic or control diet up to 14 months of age (SYN and CON, respectively). Bone mineral properties and bone strength properties can vary depending on the age of the mice with peak bone mass occurring between 4-6 months in most mice strains (Jilka 2013). It should be noted that the typical age of a mature adult mouse is 3-6 months, that the age to be considered middle-aged is 10 months, and that mice begin to show senescence changes at about 18 months of age (Flurkey et al. 2007). Thus, the mice used in this study were past development but not in a senescence stage and can be considered middle-aged. With the exception of BSL-3, humerus bones from the right side of the body were used. It has also been shown by Franco et al. that mouse humerus bones from the left side of the body have greater BMD values than those from the right (Franco et al. 2004). Storage methods have also been shown to have an influence on bone properties. Storage in ethanol, as done in this experiment, has been shown to reduce the elasticity of bone (Sedlin 1965). Genetic influences also play a role in bone phenotype and, therefore, bone properties may vary across mouse strain (Sabsovich et al. 2008). This study only analyzed the influence of the diet on male mice. Glatt et al. have detailed that female mice exhibit more

rapid bone loss than male mice (Glatt et al. 2007). Further research of the diet on female mice may reveal sex-specific influences of the diet. Therefore, the values for bone mineralization parameters as well as bone strength parameters may vary between studies due to age, genetic, sex, and bone handling influences.

We acknowledge that there are factors that prevent direct comparisons of our results with previous studies. Specifically, the humerus bones have been formalin fixed and stored for a long time in 70% alcohol, so the mechanical strength test absolute values cannot be directly compared to freshly dissected bone specimens. However, bone mineralization is well preserved so BMD comparisons can be made. Nevertheless, relative comparisons of values between the three treatment groups described in *Methods* (BSL, CON, SYN) can be made because the bones were stored in the same manner for all three groups and evaluated using the same methods and protocols. Thus, relative influences of the synbiotic diet on BMD and mechanical strength properties of the humerus can be determined.

In conclusion, this study demonstrated no enhancing effects of a long-term synbiotic diet on bone mineralization or mechanical strength in the humerus bones of adult male retired breeder mice. These findings are consistent with those of a similar study on the femur and tibia bones of the same mice (Choman, 2015). Primarily, this study has confirmed the findings of Choman. It should be noted that these findings were confirmed using a different bone (humerus vs. femur & tibia) and slightly different methodology, as Choman used micro-computed tomography to assess mineralization properties whereas a DEXA scanner was used in the present study. Furthermore, it has been demonstrated that the three-point bending machine used in the present study is appropriate for small bones from the forelimbs of mice. This expands the range of experiments that can be carried out using the three-point bending machine that was used in the present study. Lastly, this study has allowed undergraduate researchers to learn as well as develop techniques that can be applied to future projects and taught to other researchers. Regarding the findings of the synbiotic diet on the bone parameters, determining the microstructural bone response to a synbiotic diet using micro-computed tomography or histomorphology methods would facilitate a further understanding of the present findings. Furthermore, experiments investigating different animal models (e.g. female vs. male mice) could be performed to elucidate different effects across different populations.

Acknowledgements

This research was supported by the Communities to Build Active STEM Engagement (CBASE) grant at Colorado State University Pueblo. Funding from the Institute of Cannabis Research grant allowed for use of the DEXA scanner. We are grateful for the financial support. We thank Dr. Blanton at Idaho State University for providing the bone samples. We acknowledge Mr. Paul Wallace, the machine shop coordinator, for modifying the three-point bending machine, which was constructed by Mr. Paul Wallace and others at the Colorado State University Pueblo Engineering Department. Lastly, we thank the reviewers whose efforts helped improve the manuscript.

References

- Berger, A. (2002). How does it work?: Bone mineral density scans. *Bmj*, 325(7362), 484-484. doi:10.1136/bmj.325.7362.484
- Bullough, P. (1981). The geometry of diarthrodial joints, its physiologic maintenance, and the possible significance of age-related changes in geometry-to-load distribution and the development of osteoarthritis. *Clin Orthop Relat Res*, 61-66.
- Campbell, J. M., Fahey, G. C., & Wolf, B. W. (1997). Selected indigestible Oligosaccharides affect large Bowel Mass, Cecal and FECAL short-chain fatty Acids, pH and microflora in rats. *The Journal of Nutrition*, 127(1), 130-136. doi:10.1093/jn/127.1.130
- Choman, M. (2015). The Effect of a Synbiotic Diet on Bone Structure in Aging Male Mice (Unpublished master's thesis). Department of Biology, Colorado State Univeristy Pueblo.
- Coudray, C., Bellanger, J., Castiglia-Delavaud, C., Rémésy, C., Vermorel, M., & Rayssiguier, Y. (1997). Effect of soluble or partly soluble dietary fibres supplementation on absorption and balance of calcium, magnesium, iron and zinc in healthy young men. *European Journal of Clinical Nutrition*, 51(6), 375-380. doi:10.1038/sj.ejcn.1600417
- Cowin, S. C. (2009). *Bone mechanics handbook*. New York, NY: Informa Healthcare.
- Ellegård, L., Andersson, H., & Bosaeus, I. (1997). Inulin and oligofructose do not influence the absorption of cholesterol, or the excretion of cholesterol, Ca, Mg, Zn, Fe, or bile acids but increases energy excretion in ileostomy subjects. *European Journal of Clinical Nutrition*, 51(1), 1-5. doi:10.1038/sj.ejcn.1600320
- Franco, G. E., Litscher, S. J., O'Neil, T. K., Piette, M., Demant, P., & Blank, R. D. (2004). Dual Energy X Ray Absorptiometry of ex vivo HcB/Dem Mouse Long Bones: Left Are Denser Than Right. *Calcified Tissue International*, 76(1), 26-31. doi:10.1007/s00223-004-0073-5
- Freeman, J., Wopenka, B., Silva, M., & Pasteris, J. (2001). Raman Spectroscopic Detection of Changes in Bioapatite in Mouse Femora as a Function of Age and In Vitro Fluoride Treatment. *Calcified Tissue International*, 68(3), 156-162. doi:10.1007/s002230001206
- Flurkey, K., Curren, J. M., & Harrison, D. (2007). Chapter 20 - Mouse Models in Aging Research. In *The Mouse in Biomedical Research* (2nd ed., pp. 637-672). Cambridge, MA: Academic Press. doi:https://doi.org/10.1016/B978-012369454-6/50074-1
- Gibson, G. R., & Roberfroid, M. B. (1995). Dietary Modulation of the Human Colonic Microbiota: Introducing the Concept of Prebiotics. *The Journal of Nutrition*, 125(6), 1401-1412. doi:10.1093/jn/125.6.1401
- Glatt, V., Canalis, E., Stadmeier, L., & Bouxsein, M. L. (2007). Age-Related Changes in Trabecular Architecture Differ in Female and Male C57BL/6J Mice. *Journal of Bone and Mineral Research*, 22(8), 1197-1207. doi:10.1359/jbmr.070507
- Jakob, F., Seefried, L., & Schwab, M. (2014). Alter und Osteoporose. *Der Internist*, 55(7), 755-761. doi:10.1007/s00108-014-3468-z
- Jilka, R. L. (2013). The Relevance of Mouse Models for Investigating Age-Related Bone Loss in Humans. *The Journals of Gerontology Series A: Biological Sciences and Medical Sciences*, 68(10), 1209-1217. doi:10.1093/gerona/glt046
- López-Huertas, E., Teucher, B., Boza, J. J., Martínez-Férez, A., Majsak-Newman, G., Baró, L., . . . Fairweather-Tait, S. (2006). Absorption of calcium from milks enriched with fructo-oligosaccharides, caseinophosphopeptides, tricalcium phosphate, and milk solids. *The American Journal of Clinical Nutrition*, 83(2), 310-316. doi:10.1093/ajcn/83.2.310
- Sabsovich, I., Clark, J. D., Liao, G., Peltz, G., Lindsey, D. P., Jacobs, C. R., . . . Kingery, W. S. (2008). Bone microstructure and its associated genetic variability in 12 inbred mouse strains: μ CT study and in silico genome scan. *Bone*, 42(2), 439-451. doi:10.1016/j.bone.2007.09.041
- Scholz-Ahrens, K. E., Açil, Y., & Schrezenmeir, J. (2002). Effect of oligofructose or dietary calcium on repeated calcium and phosphorus balances, bone mineralization and trabecular structure in ovariectomized rats. *British Journal of Nutrition*, 88(4), 365-377. doi:10.1079/bjn2002661

- Scholz-Ahrens, K., & Schrezenmeir, J. (2002). Inulin, oligofructose and mineral metabolism — experimental data and mechanism. *British Journal of Nutrition*, 87(6), 179-186. doi:10.1079/bjbn/2002535
- Schrezenmeir, J., & Vrese, M. D. (2001). Probiotics, prebiotics, and synbiotics—approaching a definition. *The American Journal of Clinical Nutrition*, 73(2). doi:10.1093/ajcn/73.2.361s
- Sedlin, E. D. (1965). A Rheologic Model for Cortical Bone: A Study of the Physical Properties of Human Femoral Samples. *Acta Orthopaedica Scandinavica*, 36(Sup83), 1-77. doi:10.3109/ort.1965.36.suppl-83.01
- Shi, J., Lee, S., Uyeda, M., Tanjaya, J., Kim, J. K., Pan, H. C., . . . Soo, C. (2016). Guidelines for Dual Energy X-Ray Absorptiometry Analysis of Trabecular Bone-Rich Regions in Mice: Improved Precision, Accuracy, and Sensitivity for Assessing Longitudinal Bone Changes. *Tissue Engineering Part C: Methods*, 22(5), 451-463. doi:10.1089/ten.tec.2015.0383
- Silva, M. J., Brodt, M. D., Wopenka, B., Thomopoulos, S., Williams, D., Wassen, M. H., . . . Bank, R. A. (2005). Decreased Collagen Organization and Content Are Associated With Reduced Strength of Demineralized and Intact Bone in the SAMP6 Mouse. *Journal of Bone and Mineral Research*, 21(1), 78-88. doi:10.1359/jbmr.050909
- Sobolewska, A., Bogucka, J., Dankowiakowska, A., Elminowska-Wenda, G., Stadnicka, K., & Bednarczyk, M. (2017). The impact of synbiotic administration through in ovo technology on the microstructure of a broiler chicken small intestine tissue on the 1st and 42nd day of rearing. *Journal of Animal Science and Biotechnology*, 8(1). doi:10.1186/s40104-017-0193-1
- Tahiri, M., Tressol, J. C., Arnaud, J., Bornet, F. R., Bouteloup-Demange, C., Feillet-Coudray, C., . . . Coudray, C. (2003). Effect of short-chain fructooligosaccharides on intestinal calcium absorption and calcium status in postmenopausal women: A stable-isotope study. *The American Journal of Clinical Nutrition*, 77(2), 449-457. doi:10.1093/ajcn/77.2.449
- Van den Heuvel, E. G., Muys, T., Van Dokkum, W., & Schaafsma, G. (1999). Oligofructose stimulates calcium absorption in adolescents. *The American Journal of Clinical Nutrition*, 69(3), 544-548. doi:10.1093/ajcn/69.3.544
- Van den Heuvel, E. G., Schoterman, M. H., & Muijs, T. (2000). Transgalactooligosaccharides Stimulate Calcium Absorption in Postmenopausal Women. *The Journal of Nutrition*, 130(12), 2938-2942. doi:10.1093/jn/130.12.2938
- Vetter, U., Fisher, L., Mintz, K., Kopp, J., Tuross, N., Termine, J., & Robey, P. G. (2009). Osteogenesis imperfecta: Changes in noncollagenous proteins in bone. *Journal of Bone and Mineral Research*, 6(5), 501-505. doi:10.1002/jbmr.5650060512
- Wang, X., Shen, X., Li, X., & Agrawal, C. M. (2002). Age-related changes in the collagen network and toughness of bone. *Bone*, 31(1), 1-7. doi:10.1016/s8756-3282(01)00697-4
- Warming, L., Hassager, C., & Christiansen, C. (2002). Changes in Bone Mineral Density with Age in Men and Women: A Longitudinal Study. *Osteoporosis International*, 13(2), 105-112. doi:10.1007/s001980200001

Figures

Figure 1. An example of a DEXA scan experiment. (A) The Lunar Piximus II DEXA scanner that was used in the present study. (B) Humerus bones from the BSL group placed on the artificial tissue block with a cotton thread and numbered label tied around them. (C) A single mouse humerus bone captured by the Lunar Piximus II DEXA scanner and enclosed in a ROI (red) for analysis. (D) A data report for the humerus bone shown in panel C.

Figure 2. The three-point bending machine utilized in the present study. (A) The three-point bending machine imaged with deflection meter and force sensor. (B) A humerus bone on a two-beam support with crosshead beam at the midshaft.

Figure 3. A representative force-deflection curve for a 3-point bending test on a mouse humerus bone. The curves were generated and analyzed using waveform analysis tools in Igor Pro 6.36. Cursor pairs were placed on the force-displacement curve to mark regions of interest. The entire curve is bound by cursors A and B. Cursors C and D identify the linear elastic region, the portion of the curve where the bone will return to its original shape if the force is removed. Cursor E marks the yield point, the point beyond which the bone becomes plastic, where it will not return to its original shape if the force is removed. Cursors G and H bracket the ultimate force. Cursors I and J bracket the fracture force region.